Inorganic Chemistry

Forum Article

pubs.acs.org/IC

Cyclometalated Iridium(III) Complexes for Phosphorescence Sensing of Biological Metal Ions

Youngmin You,*[,†] Somin Cho,[‡] and Wonwoo Nam*[,‡]

[†]Department of Advanced Materials Engineering for Information and Electronics, Kyung Hee University, 1 Seocheon-dong, Giheung-gu, Yongin-si, Gyeonggi-do 446-701, Korea

[‡]Department of Bioinspired Science and Department of Chemistry and Nano Science, Ewha Womans University, Daehyun-dong, Seodaemun-gu, Seoul 120-750, Korea

Supporting Information

ABSTRACT: Phosphorescence signaling provides a valuable alternative to conventional bioimaging based on fluorescence. The benefits of using phosphorescent molecules include improved sensitivity and capabilities for effective elimination of background signals by time-gated acquisition. Cyclometalated Ir(III) complexes are promising candidates for facilitating phosphorescent bioimaging because they provide synthetic versatility and excellent phosphorescence properties. In this Forum Article, we present our recent studies on the development of phosphorescence sensors for the detection of metal ions based on cyclometalated iridium(III) complexes. The constructs contained cyclometalating (C^N) ligands with the electron densities and band-gap energies of the C^N ligand structures systematically varied. Receptors that chelated zinc, cupric, and chromium ions were tethered to the ligands to create phosphorescence sensors. The alterations in the C^N ligand structures had a profound influence on the phosphorescence responses to metal ions. Mechanistic studies suggested that the phosphorescence responses could be explained on the basis of the modulation of photoinduced electron transfer (PeT) from the receptor to the photoexcited iridium species. The PeT behaviors strictly adhered to the Rehm−Weller principle, and the occurrence of PeT was located in the Marcus-normal region. It is thus anticipated that improved responses will be obtainable by increasing the excited-state reduction potential of the iridium(III) complexes. Femtosecond transient absorption experiments provided evidence for the presence of an additional photophysical mechanism that involved metal-ion-induced alteration of the intraligand charge-transfer (ILCT) transition state. Utility of the mechanism by PeT and ILCT has been demonstrated for the phosphorescence sensing of biologically important transition-metal ions. In particular, the phosphorescence zinc sensor could report the presence of intracellular zinc pools by using confocal laser scanning microscopy and photoluminescence lifetime imaging microscopy techniques. We hope that the significant knowledge gained from our studies will be of great help in the design of new molecules as phosphorescence sensors.

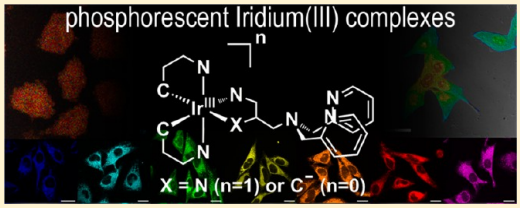

INTRODUCTION

Biological research has benefited greatly from advances in photoluminescence imaging techniques based on molecular probes. A variety of fluorescent molecules have served as probes for visualization of many important entities at cellular and organismal levels. For instance, fluorescent sensors were employed in elucidating signaling processes mediated by calcium[1,2] and zinc ions.[3−6] The benefits of using fluorescent probes are enormous; excellent spatiotemporal resolution can be attainable with the minimum dosage of the compounds. More importantly, the knowledge that has been accumulated about the synthetic tuning and spectroscopic techniques of molecular photoluminescence provides exceptional versatility.

It has been recognized that phosphorescence bioimaging could be a promising alternative to fluorescence techniques because long-lifetime phosphorescence emission can easily be discriminated from background noise caused by autofluorescence and scattered light. Notably, NADH, a coenzyme existing at millimolar levels in mammalian cells, exhibits broad fluorescence emission ranging from 400 to 600 nm.[7] In addition, many endogenous chromophoric species exist, including flavins, metal-free porphyrins, and components of lipofuscin, elastin, and keratin. These fluorescent biomolecules reduce the signal-to-noise ratios, limiting the reliability of fluorescence bioimaging. Because fluorescence noise has a considerably shorter emission lifetime (<100 ns) than that of phosphorescence emission (ca. microseconds), gated phosphorescence acquisition at 100 ns delay can completely eliminate the noise. This idea has recently been demonstrated for bioimaging based on long-lifetime emitters such as lanthanide complexes.[8−14]

Despite these advantages, phosphorescence bioimaging has been significantly held back by a lack of high-efficiency room temperature phosphorescent molecules. The recent development of phosphorescent transition-metal complexes, such as those containing platinum(II) and iridium(III),[15] for use in

Special Issue: Imaging and Sensing

Received: June 1, 2013
Published: November 22, 2013

   dx.doi.org/10.1021/ic4013872 | Inorg. Chem. 2014, 53, 1804−1815

Scheme 1. Structures of Biscyclometalated Iridium(III) Complexes Having Different Cyclometalating Ligands

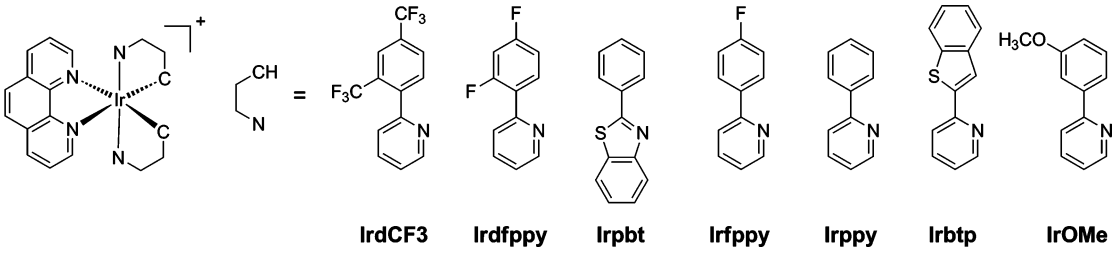

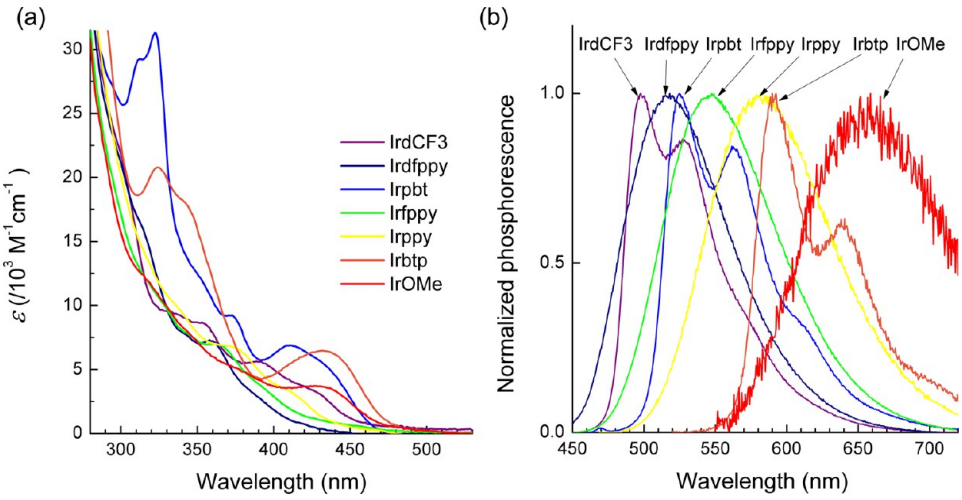

Figure 1. (a) UV−vis absorption and (b) normalized phosphorescence spectra of iridium(III) complexes (10 μM, argon-saturated CH_3CN) at room temperature.

electroluminescence has inspired new approaches to bioimaging.[16−35] Among the transition-metal complexes, cyclometalated iridium(III) complexes have emerged as promising candidates for use as phosphorescence sensors because of their high phosphorescence quantum yields (Φ_p) and the ability for wide spectral tuning.[17,36−41] Several pioneering research groups have already demonstrated the potential use of cyclometalated iridium(III) complexes for phosphorescent staining of intracellular organelles, including nuclei,[42,43] mitochondria,[44] lysosomes,[45] endoplasmic reticuli,[46,47] plasma membranes,[44,48] and cytoplasms.[42,44,46,47,49,50] More details on phosphorescent bioimaging including cellular staining using cyclometalated iridium(III) complexes can be found in recent reviews.[36,51−60]

In contrast to the success of using iridium(III) complexes in cellular staining applications, phosphorescence biosensors based on such compounds are relatively underdeveloped. Although recent reports on the detection of metal ions,[16,17,20,21,28−30,33,34,60−65] oxygen,[66−69] anions,[70] and biological molecules, such as DNA,[71,72] amino acids,[73−79] and glucose,[80] have gained increasing interest, examples of successful applications in vitro/in vivo remain sparse. This scarcity may reflect our poor understanding of the principles underlying the phosphorescence responses to the analytes. For instance, tethering a metal chelator, di-2-picolylamine (DPA), to 1,10-phenanthroline (phen) and 4,4′-distyryl-2,2′-bipyridine ligands of cyclometalated iridium(III) complexes produced different responses.[63−65] To maximize biosensing capabilities of the iridium(III) complexes, gaining an in-depth understanding of the molecular principles of phosphorescence control is of crucial importance. In this Forum Article, we disclose our recent strategies to the creation of phosphorescence sensors of biometals utilizing cyclometalated iridium(III) complexes. We hope that the knowledge gained from our studies will provide useful insight for the future development of phosphorescence sensors.

MOLECULAR DESIGN OF PHOSPHORESCENCE SENSORS

Phosphorescence emission of the cyclometalated iridium(III) complexes is characterized with high quantum yields. The high efficiencies are due to the strong spin−orbit coupling provided by the iridium core, which enables the nonzero transition probability to overcome the spin restriction of phosphorescence transition. It is noted that the one-electron spin−orbit coupling constant of iridium(III) (ζ_{SOC} = 3909 cm^{-1}) is greater than that of ruthenium(II) (ζ_{SOC} = 990 cm^{-1}).[81,82] Further details surrounding the photophysics of phosphorescent iridium(III) complexes can be found in recent reviews.[40,41,83−85] To systematically investigate control of the phosphorescence properties by variations in the ligand structures, a series of cyclometalated iridium(III) complexes with the general formula $[Ir(C^N)_2phen]^+$ (C^N = cyclometalating ligand) were chosen (Scheme 1).[86] Seven C^N ligands were employed, namely, 2-[2,4-bis(trifluoromethyl)phenyl]pyridine, 2-(2,4-difluorophenyl)pyridine, 2-(4-fluorophenyl)pyridine, 2-phenylbenzothiazole, 2-phenylpyridine (ppy), 2-(2-benzo[*b*]thienyl)-pyridine (btp), and 2-(3-methoxyphenyl)pyridine.

As shown in Figure 1a, the UV−vis absorption spectra of the $[Ir(C^N)_2phen]^+$ complexes can be seen to be characterized by the presence of multiple bands that involve the high-energy ligand-centered transition bands (<350 nm) and the relatively low-energy metal-to-ligand charge-transfer (MLCT) transition

dx.doi.org/10.1021/ic4013872 | *Inorg. Chem.* 2014, 53, 1804−1815

Scheme 2. Syntheses and Structures of the Phosphorescent Sensors for Metal Ions

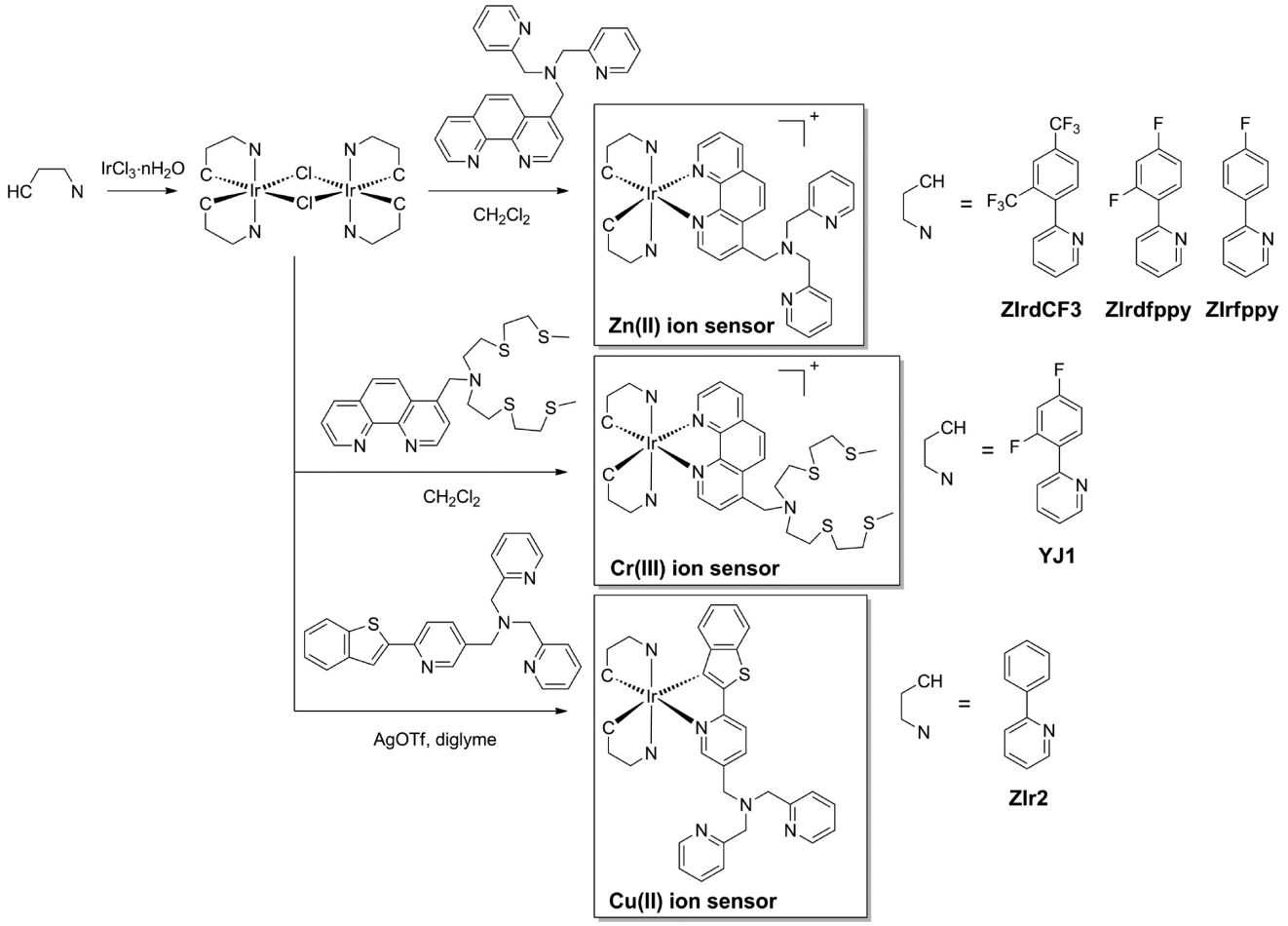

bands (350−450 nm).[87] The peak wavelength of the singlet MLCT (^{1}MLCT) absorption band increases in the following order: Irdfppy (388 nm) > IrdCF3 (393 nm) > Irfppy (394 nm) > Irpbt (407 nm) > Irppy (409 nm) > Irbtp (431 nm) > IrOMe (436 nm). This order can be qualitatively correlated to the electron densities of the C^N ligands, revealing the strong influence of the C^N ligands on the MLCT transition energies.

Photoexcitation at the MLCT transition bands provokes strong room temperature phosphorescence emission. The phosphorescence quantum yields range from 0.21% to 23% in degassed CH_3CN solutions [Supporting Information (SI), Table S1]. As shown in Figure 1b, the C^N ligand variations produce color-tuned phosphorescence over a wide spectral range of 499−650 nm. The phosphorescence peak wavelengths of the iridium(III) complexes increase in an order similar to that for the ^{1}MLCT absorption bands (see the SI, Table S1), suggesting that the MLCT transition state is responsible for phosphorescence emission. This assignment is supported by the linear dependence between the phosphorescence energy versus the redox gap of the $Ir^{III/IV}$ oxidation [$E_{1/2}(Ir^{III/IV})$ = 0.94−1.70 V vs SCE] and the phen ligand reduction (E_{red} ∼ −1.26 V vs SCE) (SI, Figures S1 and S2).

The photophysical properties present several challenges for applying a cyclometalated iridium(III) complex to bioimaging. The MLCT transition band exhibits molar absorbance values (ε < 10^4 M^{-1} cm^{-1}) lower than those of typical organic fluorophores, such as fluorescein (ε ∼ 10^4−10^5 M^{-1} cm^{-1}). This weak light absorption would significantly limit the brightness. In addition, the MLCT bands remain in the UV or near-UV regions, so the depth of penetration would not be enough to allow visualization at the organismal levels. Although multiphoton phosphorescence microscopy can overcome these drawbacks, future research into improving the absorption properties is urgently required.

Nevertheless, high-efficiency room temperature phosphorescence encourages the use of biscyclometalated iridium(III) complexes for sensing applications for the detection of biological metal ions, such as labile zinc. Because the zinc(II) ion itself has no spectroscopic signature because of its fully filled d^{10} electronic configuration, phosphorescence signaling on zinc-ion recognition would rely on photophysical communication between the iridium(III) complex and a zinc-ion receptor. DPA is frequently chosen as the zinc-ion receptor because it has a strong affinity to divalent transition-metal ions over biologically abundant alkali- and alkaline-earth-metal ions.[5] Although the Irving−Williams series predicts a greater binding preference for copper(II) ions over zinc(II) ions, considerably higher concentrations of labile zinc preclude artifacts due to copper(II) ions.[88−94] The molecular design of phosphorescence zinc sensors can involve the attachment of DPA at the ligand peripheries of the iridium(III) complexes. In such dyad structures, photoexcitation of the MLCT transition band would promote photoinduced electron transfer (PeT) from DPA to the photoexcited iridium species because of the higher oxidation potential of DPA (E_{ox} = 1.28 V vs SCE),[86] effectively suppressing the radiative transition of the iridium(III) complex. Zinc-ion binding to DPA would

dx.doi.org/10.1021/ic4013872 | Inorg. Chem. 2014, 53, 1804−1815

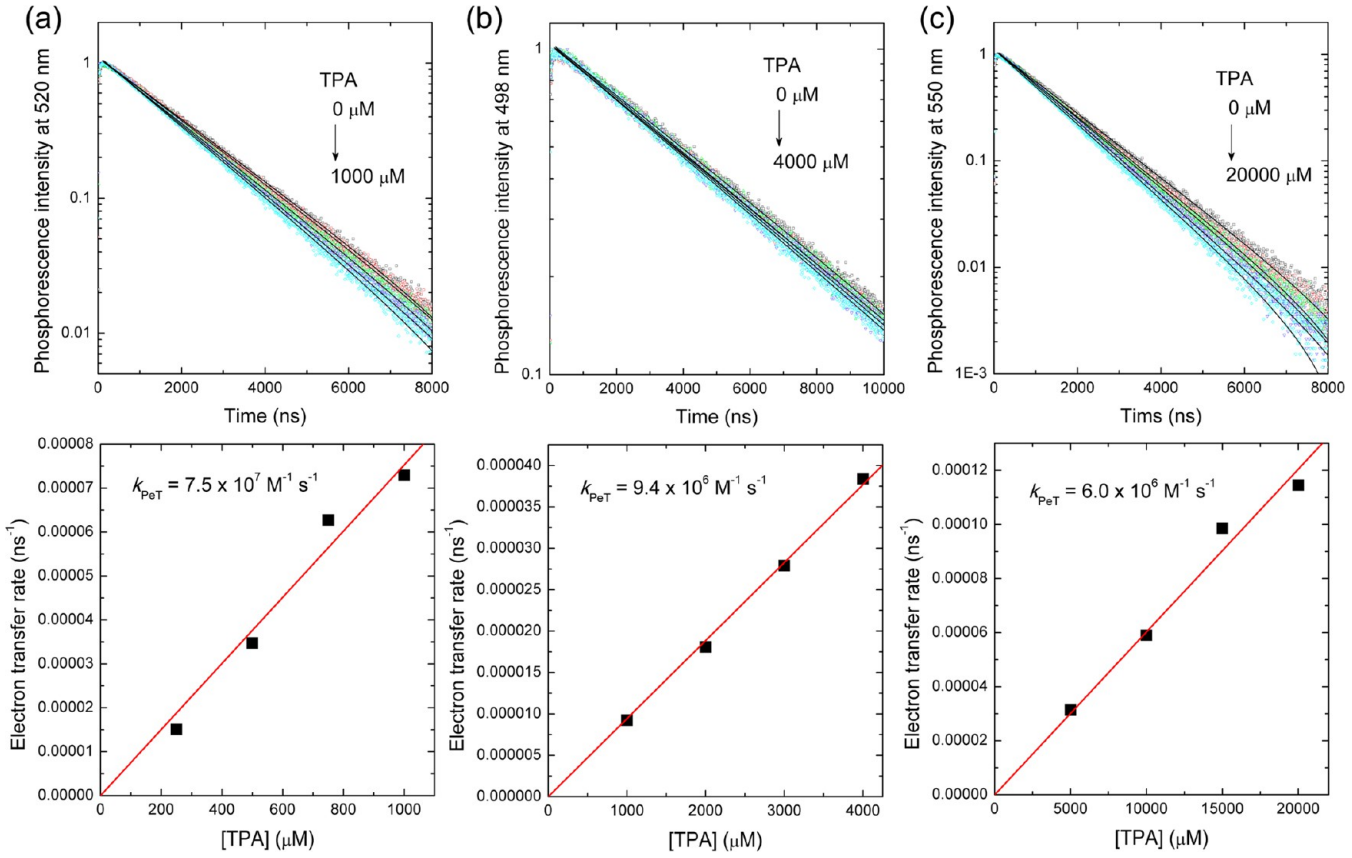

Figure 2. Determination of the bimolecular rate constants for PeT (k_{PeT}) from TPA to iridium complexes upon nanosecond-pulsed photoexcitation at λ = 377 nm: (a) Irdfppy; (b) IrdCF3; (c) Irfppy. Top panels: phosphorescence decay traces of 100 μM iridium complexes in argon-saturated CH_3CN solutions containing increasing concentrations of TPA (λ_{obs}: Irdfppy, 520 nm; IrdCF3, 498 nm; Irfppy, 550 nm). Lower panels: plot of the electron-transfer rate as a function of the TPA concentration. The electron-transfer rate was calculated by the relationship electron-transfer rate = $1/\tau - 1/\tau_0$, where τ and τ_0 are the phosphorescence lifetimes of the iridium complex in the presence and absence of TPA, respectively. The slope corresponds to k_{PeT}.

reduce the electron-donating ability of DPA to restore the inherent phosphorescence emission. Thus, the overall response to zinc ions is phosphorescence turn-on.

To validate the effectiveness of PeT from DPA to the series of biscyclometalated iridium(III) complexes, we conducted phosphorescence quenching experiments. Tri-2-picolylamine (TPA), instead of DPA, was employed as the electron donor to mimic the structure of the DPA moiety attached to an iridium(III) complex (see Scheme 2). Phosphorescence decays of the iridium(III) complexes (100 μM in argon-saturated CH_3CN) after 377 nm nanosecond-pulsed laser excitation were monitored with increasing TPA concentrations (Figure 2). TPA affected the phosphorescence decays of Irdfppy, IrdCF3, and Irfppy, whereas the decay traces of other complexes were unaffected by the presence of TPA. We thus determined the bimolecular rate constants for PeT (k_{PeT}) from TPA to Irdfppy, IrdCF3, and Irfppy to be 7.5 × 10^7, 9.4 × 10^6, and 6.0 × 10^6 M^{-1} s^{-1}, respectively (Figure 2). It is noted that the k_{PeT} value increases in proportion with the driving force for PeT, $-\Delta G_{PeT} = e[E_{ox}(TPA) - E^*_{red}(Ir)]$, where e, E_{ox}(TPA), and E^*_{red}(Ir) are the elementary charge, the oxidation potential of TPA (1.28 V vs SCE), and the excited-state reduction potential of the iridium(III) complex. E^*_{red}(Ir) values were calculated by E_{red}(Ir) + ΔE_{00}, where E_{red}(Ir) and ΔE_{00} are the ground-state reduction potential and the band-gap energy of the iridium complexes (see the SI, Table S1). Figure 3 displays the positive dependence of k_{PeT} to $-\Delta G_{PeT}$ of the iridium(III) complexes, which is typical of electron transfer

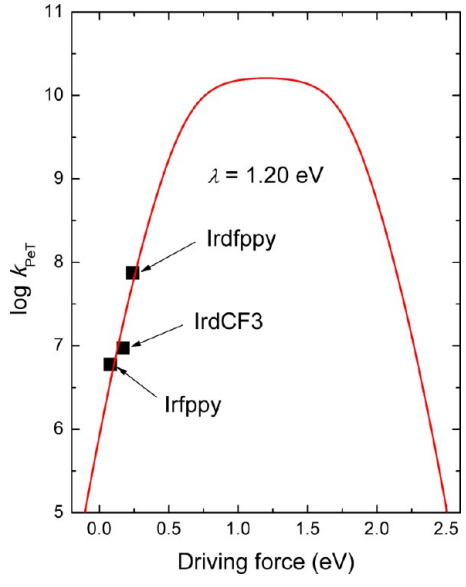

Figure 3. Plot of log k_{PeT} versus the driving force for PeT from TPA to the photoexcited species of the iridium complexes. The red curve is a theoretical plot of eq 1 with a reorganization energy λ of 1.20 eV.

occurring in the Marcus-normal region. The k_{PeT} values can be fitted to the theoretical equation for adiabatic electron transfer of

dx.doi.org/10.1021/ic4013872 | Inorg. Chem. 2014, 53, 1804−1815

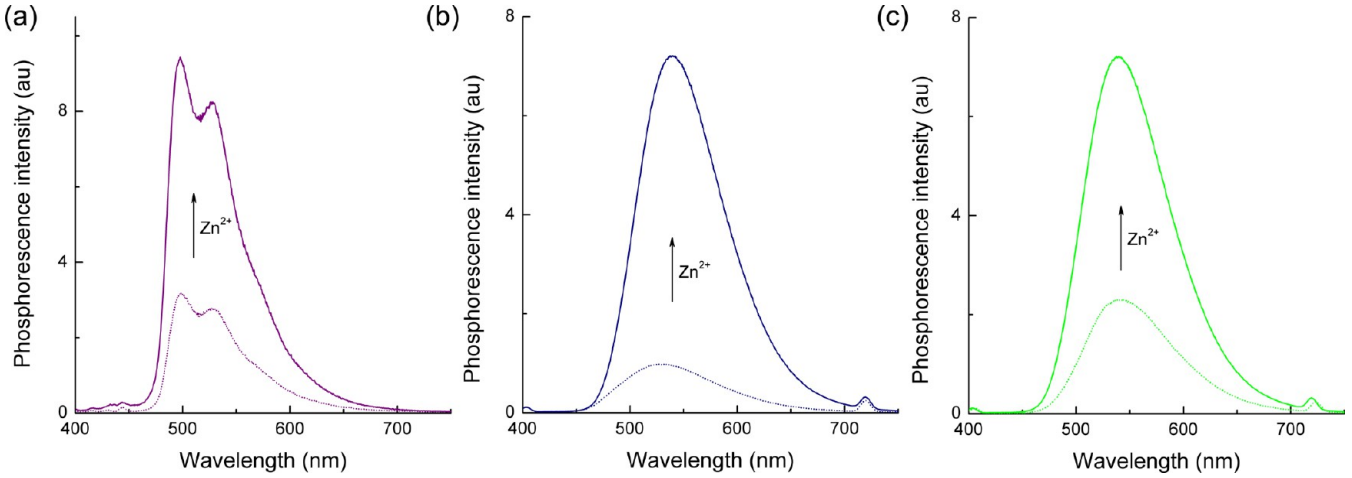

Figure 4. Phosphorescence responses of iridium(III) complexes (10 μM in deaerated CH_3CN) to zinc ions [3 equiv of $Zn(ClO_4)_2$]: (a) ZIrdCF3; (b) ZIrdfppy; (c) ZIrfppy. For more details, see ref 86.

the Marcus theory after diffusion processes between TPA and the iridium(III) complex are taken into account (eq 1):[95]

$$k_{PeT} = \frac{k_{diff}k_{eT}}{k_{-diff} + k_{eT}} = \frac{k_{diff}Z\ \exp[-(\Delta G_{PeT} + \lambda)^2/4\lambda k_B T]}{k_{-diff} + Z\ \exp[-(\Delta G_{PeT} + \lambda)^2/4\lambda k_B T]} \quad (1)$$

In eq 1, Z and λ are the collisional frequency taken as 1.0×10^{11} M^{-1} s^{-1} and the reorganization energy for the one-electron transfer, respectively. The diffusion rate constant (k_{diff}) in CH_3CN at 298 K, 1.93×10^{10} M^{-1} s^{-1}, was calculated by the Stokes–Einstein–Smoluchowski equation, $k_{diff} = 8k_BN_AT/3\eta$, where k_B, N_A, T, and η are the Boltzmann constant, Avogadro's number, the absolute temperature, and the viscosity of the solvent, respectively. Iterations of nonlinear least-squares fits to eq 1 returned a λ value of 1.20 eV. Because the $-\Delta G_{PeT}$ values (0.19 eV for Irdfppy, 0.16 eV for IrdCF3, and 0.05 eV for Irfppy) are significantly smaller than 1.20 eV, increasing the driving force can potentially improve the PeT rates. Zinc coordination attenuates the electron-donating ability of TPA, restoring phosphorescence emission.

SYNTHESES OF THE PHOSPHORESCENCE SENSORS BASED ON IRIDIUM(III) COMPLEXES

The modulation of PeT by zinc coordination is highly advantageous for sensing applications because the response is prompt and fully reversible. In addition, the turn-on response is specific to zinc(II) ions over other competing paramagnetic transition-metal ions, such as copper(II) and iron(II). Taking advantage of PeT, a broad range of biologically applicable fluorescent zinc-ion sensors have been successfully developed to date, including the attachment of DPA to fluorescent chromophores such as coumarin,[96,97] fluorescein,[98−113] quinoline,[114−120] and hydroxybenzoxazole.[121−125] The sensors have found wide bioimaging utility in visualization of labile zinc in synaptic vesicles and apoptotic cells.[3−5,126−130] These previous studies present the potential of phosphorescent zinc-ion sensors consisting of DPA and iridium(III) complexes. On the basis of this consideration, we have constructed three phosphorescence zinc-ion sensors, ZIrdfppy, ZIrdCF3, and ZIrfppy (Scheme 2).[63,86] DPA can be introduced at the 4 position of the phen ligand through a methylene linker. The broken conjugation between DPA and phen removes the possibilities of electronic communication, allowing for phosphorescence responses governed solely by PeT. Scheme 2 summarizes the synthetic routes to the preparation of phosphorescent sensors for the detection of zinc ions. The principle has also been applied to create phosphorescence sensors for chromium ions (YJ1 in Scheme 2) and cupric ions (ZIr2 in Scheme 2). The heteroleptic iridium(III) complexes are typically prepared through a standard two-step procedure involving use of the Nonoyama reaction to prepare a bis(μ-Cl)Ir^{III} dimer,[131] followed by substitution of the chlorides with the third ligand (phen or C^N ligand). Subsequent metathesis with NH_4PF_6 enables the resulting $[Ir(C^N)_2phen]PF_6$ to be treated using standard organic synthesis methods, including silica gel column purification. The metal-ion receptors can be readily incorporated into the phen ligand, through SeO_2-mediated oxidation of 4-methyl-1,10-phenanthroline, followed by reductive amination with the secondary amines that carry metal-coordinating entities.[63,86] Attaching the receptors to the C^N ligands is challenging because the Nonoyama reaction exhibits extremely poor tolerance to the presence of metal-coordinating moieties, and the high reaction temperature necessary for cyclometalation frequently results in cleavage of the receptors. For instance, cyclometalation of the 2-(2-pyripyl)benzo[*b*]thiophene (btp) ligand having the DPA moiety to a biscyclometalated iridium core proceeds with low yield.[62]

PHOSPHORESCENCE RESPONSES AND PHOTOPHYSICAL MECHANISMS

The phosphorescence spectra of the zinc-ion sensors (i.e., ZIrdfppy, ZIrdCF3, and ZIrfppy) are almost identical with those of their parent complexes (i.e., Irdfppy, IrdCF3, and Irfppy; Figures 1b and 4), apart from significant decreases in the phosphorescence quantum yields (Φ_p) for ZIrdfppy (0.45%), ZIrdCF3 (1.4%), and ZIrfppy (3.0%). These particular iridium(III) complexes show phosphorescence turn-on responses (Figure 4), with their phosphorescence turn-on ratios quantified by dynamic range (DR) values [$\Phi_p(Zn^{2+})/\Phi_p(Zn^{2+}$-free)] to be 31, 12, and 2.9 for ZIrdfppy, ZIrdCF3, and ZIrfppy, respectively. The shape of the phosphorescence spectra does not vary upon zinc-ion coordination; however, small bathochromic shifts are observed for ZIrdfppy (529 cm^{-1}) and ZIrfppy (805 cm^{-1}). The similarities in the phosphorescence spectra before and after zinc-

dx.doi.org/10.1021/ic4013872 | Inorg. Chem. 2014, 53, 1804−1815

ion binding suggest that the triplet states responsible for phosphorescence are identical.

It is especially noted that the DR values follow the order of ZIrdfppy > ZIrdCF3 > ZIrfppy, which is consistent with the trend in the k_{PeT} values determined for their parent complexes (Figure 3). Indeed, as shown in Figure 5, a positive correlation

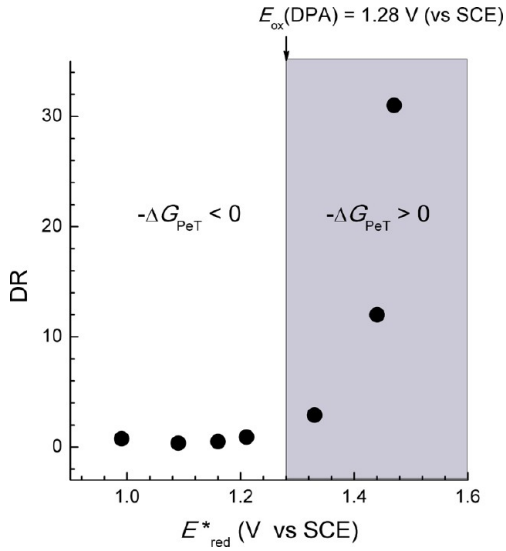

Figure 5. Plot of DR versus E^*_{red} of the phosphorescence zinc-ion sensors. For more details, see ref 86.

between the DR and E^*_{red}(Ir) values is clearly evident, with larger DR values obtained for iridium(III) complexes with larger E^*_{red}(Ir) values. Considering the narrow range in E_{red} values for the series of iridium(III) complexes (SI, Table S1), it is concluded that the major molecular parameter governing PeT is ΔE_{00}. However, it should be noted that E^*_{red}(Ir), not ΔE_{00}, is directly correlated with the occurrence of PeT. The intramolecular PeT rate, calculated from PeT rate = (DR − 1)/τ_0,[132,133] ranges from 1.44×10^6 s^{-1} (ZIrfppy) to 1.56×10^7 s^{-1} (ZIrdfppy). These values are again proportional to the $-\Delta G_{PeT}$ values, suggesting that PeT occurs in the Marcus-normal region.

Femtosecond laser flash photolysis studies suggest an additional mechanism for the phosphorescence turn-on response of the zinc probes.[63] As shown in Figure 6a, the transient absorption spectrum of Irdfppy features absorption bands at 540 and 1100 nm. These bands are characteristic of the phen radical anion (phen$^{\bullet-}$), indicating generation of the MLCT transition state involving the phen ligand ($ML_{N^\wedge N}CT$). For the zinc-free form of ZIrdfppy, the peaks due to phen$^{\bullet-}$ can be seen to be hypsochromically shifted to 530 and 1000 nm (Figure 6b), which suggests a different origin for the charge-transfer state. Because DPA is more easily oxidized than the iridium(III) center (1.28 vs 1.56 V vs SCE), the signatures of phen$^{\bullet-}$ of zinc-free ZIrdfppy may result from charge transfer from DPA. Thus, it is reasonable to assign the electronic state involving phen$^{\bullet-}$ to the intraligand charge-transfer ($IL_{N^\wedge N}CT$; i.e., DPA → phen charge transfer) transition state of the DPA-appended phen ligand. The weak phosphorescence intensity of ZIrdfppy can therefore be attributed to the presence of the $IL_{N^\wedge N}CT$ transition state because the ILCT transition is typically characterized by weak emission intensities.[134−140] Zinc-ion binding restores the $ML_{N^\wedge N}CT$ transition state, as observed in Figure 6c. The near-IR $IL_{N^\wedge N}CT$ absorption band (1000 nm) converts to the $ML_{N^\wedge N}CT$ absorption band (1100 nm) after 20 ps, which may explain the phosphorescence turn-on. Taking these results into account, the mechanism for the phosphorescence turn-on by zinc-ion binding is summarized in Scheme 3. Photoexcitation promotes prompt reductive electron transfer to the phen ligand. Two electron donors, DPA and the iridium(III) core, exist, which lead to the $IL_{N^\wedge N}CT$ and $ML_{N^\wedge N}CT$ transition states, respectively, with nonradiative transition facilitated through the former. In the case of the $ML_{N^\wedge N}CT$ transition state, phosphorescence emission is effectively quenched by PeT from DPA to the transiently generated iridium(IV) species. The intramolecular PeT occurs at rates of 10^6−10^7 s^{-1}, being far faster than the radiative transitions (10^4−10^5 s^{-1}; see the SI, Table S1) in the complexes. Thus, the overall effect is phosphorescence turn-off. Zinc-ion binding at DPA shuts down these phosphorescence quenching routes, producing phosphorescence turn-on.

It is noted that the extent of $IL_{N^\wedge N}CT$ and PeT in the iridium(III) complexes varies, with the ligand structures having a profound influence on the extent of phosphorescence quenching. For instance, phosphorescence turn-off by DPA is not observed for the triscyclometalated heteroleptic iridium(III) complex, ZIr2 (Figure 7).[62] The incorporation of the electron-rich btp C^N ligand instead of the phen ligand abolishes PeT. The detailed photophysical mechanism has yet to be fully elucidated, but the absence of phosphorescence quenching in the metal-free form of ZIr2 can be reasonably ascribed to suppression of PeT from DPA. Interestingly, dual phosphorescence emission is observed presumably because of weak electronic communication between two separate ligands. ppy and btp ligands produce green and red emission bands in the ranges of 470−570 and 580−700 nm, respectively (Figure 7). Coordination of paramagnetic copper(II) ions to DPA preferentially quenches phosphorescence emission from the btp ligand. This phosphorescence behavior can be utilized for visualization of intracellular cupric ions in HeLa cells.

Another effect of metal-ion binding to DPA is the bathochromic shift in the phosphorescence spectra (Figure 4). These shifts are deduced to originate from the positive charge of the metal ions because identical shifts are found when other Lewis acids, such as scandium(III) ions, are added.[86] It is likely that the extra charge provides an additional stabilization effect on the charge-transfer state. This effect is not limited to the DPA-appended iridium(III) complexes; a similar ratiometric phosphorescence change is observed for Irdfppy having a bis(thioether)amino receptor at the phen ligand (Figure 8).[61] The addition of chromium(III) ions into acetonitrile solutions of the iridium(III) complex leads to phosphorescence turn-on with a significant red shift. This phosphorescence response can be explained on the basis of the combined effect of extra positive charge and suppression of $IL_{N^\wedge N}CT$ and PeT. Interestingly, air equilibration of the acetonitrile solution restores the phosphorescence color. The second phosphorescence ratiometric response is due to a biomimetic oxidation reaction by dioxygen (O_2) activation of the chromium(III) center (see Figure 8). To the best of our knowledge, the phosphorescence chromium(III) probe is the first system demonstrated to possess a dual-stage ratiometric response.

APPLICATIONS TO VISUALIZATION OF LABILE ZINC IONS

The phosphorescence zinc sensor, ZIrdfppy, retains its phosphorescence zinc-ion sensing capabilities in buffered aqueous solutions (pH 7.0, 25 mM PIPES). The phosphorescence turn-on response of the probe is barely affected by the

dx.doi.org/10.1021/ic4013872 | Inorg. Chem. 2014, 53, 1804−1815

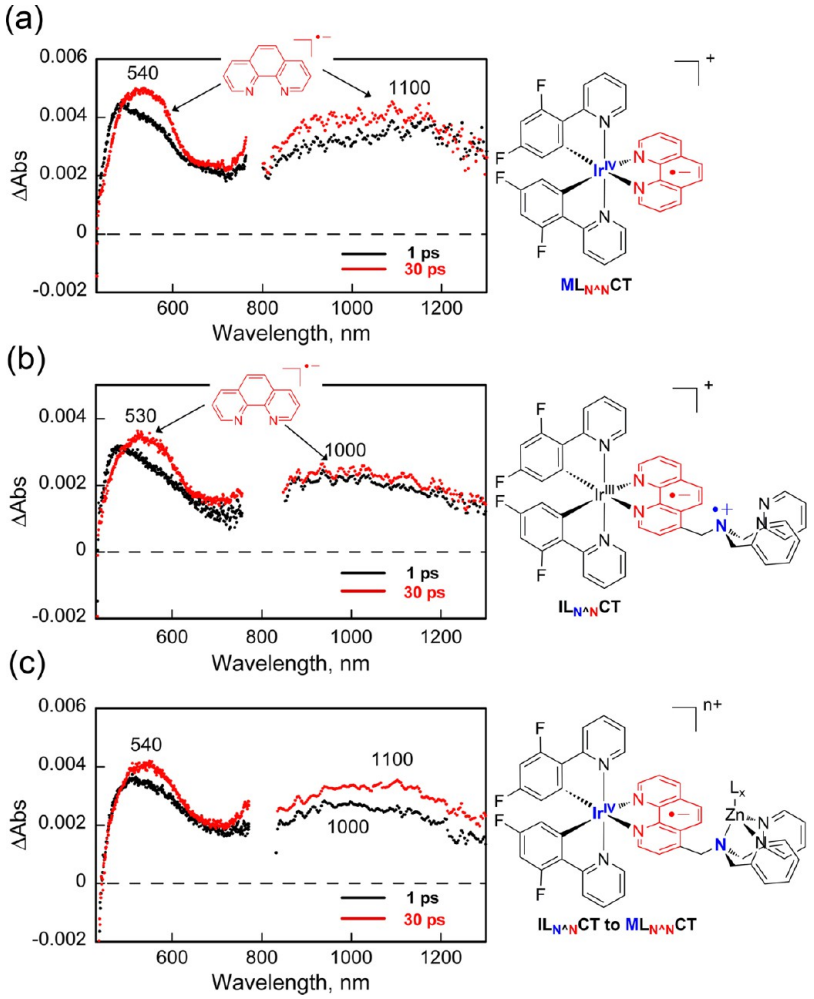

Figure 6. Femtosecond transient absorption spectra measured at 1 ps (black curves) and 30 ps (red curves) delay after photoexcitation at 420 nm: (a) 0.30 mM Irdfppy; (b) zinc-free form of 0.30 mM ZIrdfppy; (c) zinc-bound form of 0.30 mM ZIrdfppy (1.0 mM zinc ion). Reprinted with permission from ref 63. Copyright 2011 American Chemical Society.

pH change in the range of 5.1−10.0 (SI, Figure S3), as is also determined by the low pK_a value (pK_a = 4.42).[63] An apparent zinc-ion dissociation constant (K_d) is as low as 11 nM, and the phosphorescence zinc-ion response is fully reversible and not influenced by physiologically abundant alkali- and alkaline-earth-metal ions, including Na^+, Mg^{2+}, K^+, and Ca^{2+}, and biological transition-metal ions, such as Mn^{2+}, Fe^{2+}, Ni^{2+}, Co^{2+}, and Cu^{2+} (see ref 63 for details).

ZIrdfppy readily enters live HeLa cells when the cells are incubated at 37 °C with media containing 5−10 μM ZIrdfppy. On the contrary, treatments of the cells at 4 °C significantly retard the uptake of ZIrdfppy, as seen by the lower phosphorescence intensities in the microscopic images (SI, Figure S4). Thus, the intracellular entry of the zinc probe may involve active transport mechanisms. Colocalization experiments with organelle-specific stains, MitoTracker Deep Red FM, Hoechst 33258, LysoTracker Red, and ER−Tracker Blue−White DPX, revealed localization of ZIrdfppy within the mitochondria of HeLa cells (Figure 9). Because labile zinc pools in mitochondria have been recognized in a broad range of mammalian cells,[141,142] the localization ability of the probe will be valuable to investigations of the biological mechanisms of mitochondrial zinc.

Figure 10a displays confocal laser scanning microscopy images of live A549 cells preincubated with 5 μM ZIrdfppy.[63] The treated cells initially exhibit weak phosphorescence, but the subsequent addition of zinc ionophore, $ZnCl_2$/NaPT (ZnPT), turns on phosphorescence. As expected for a zinc-ion sensor, treatment with a strong zinc-ion chelator, *N*,*N*,*N*′,*N*′-tetrakis(2-picolyl)ethylenediamine (TPEN), restores the lower phosphorescence intensity. Such successful monitoring of the cellular flux of zinc ions suggests that the sensing utility can be potentially extended to visualization of zinc-ion-rich specimens, such as the hippocampus.

Photoluminescence lifetime imaging microscopy experiments demonstrate the advantages of long-lifetime photoluminescence signaling. Figure 10b shows photoluminescence lifetime micrographs (80 μm × 80 μm area) of HeLa cells incubated with ZIrdfppy in the absence and presence of $ZnCl_2$/NaPT. A photoluminescence decay trace collected at each pixel can be fitted to a three-exponential model to yield short, midrange, and long-lifetime components. The short and midrange time constants are less than 10 ns and independent of the presence of zinc ions.[63] In contrast, the long-lifetime component is increased by the zinc treatment, suggesting that this particular component corresponds to phosphorescence signaling.

dx.doi.org/10.1021/ic4013872 | *Inorg. Chem.* 2014, 53, 1804−1815

Scheme 3. Proposed Photophysical Mechanism for Phosphorescence Signaling

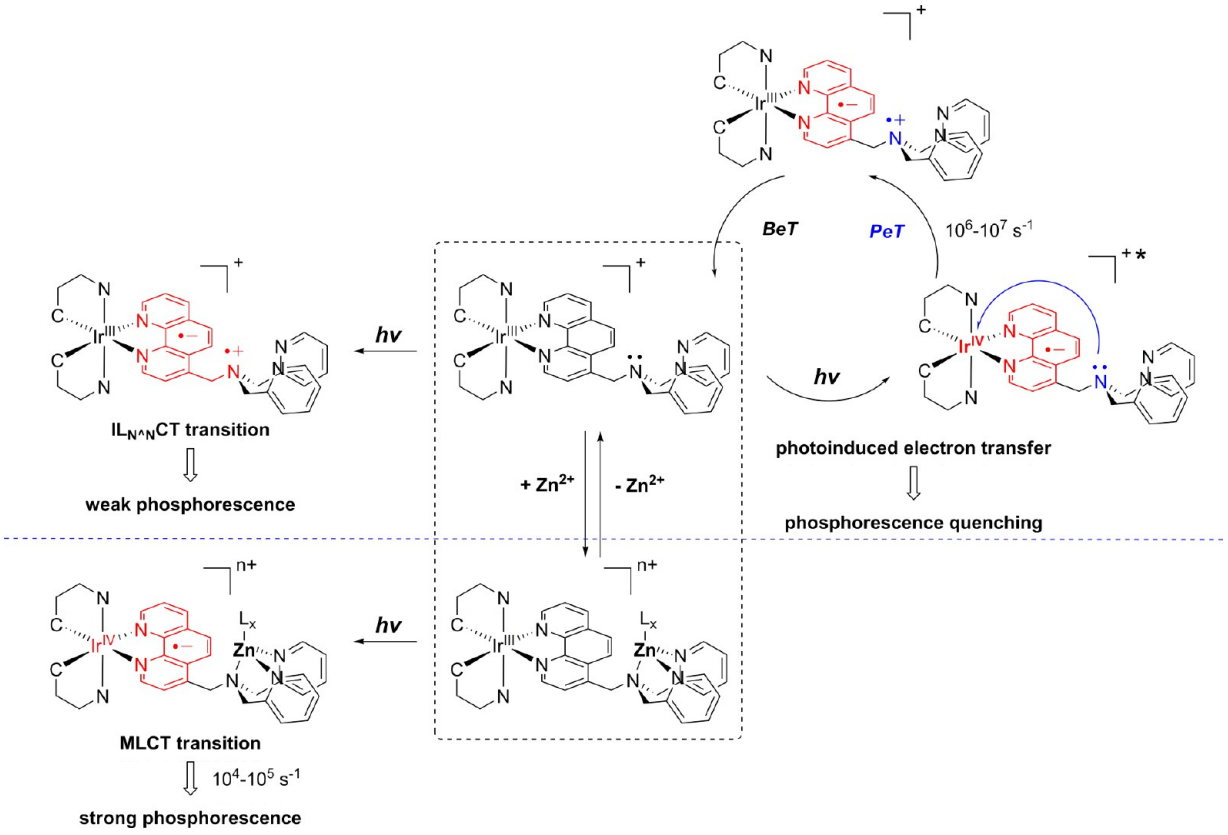

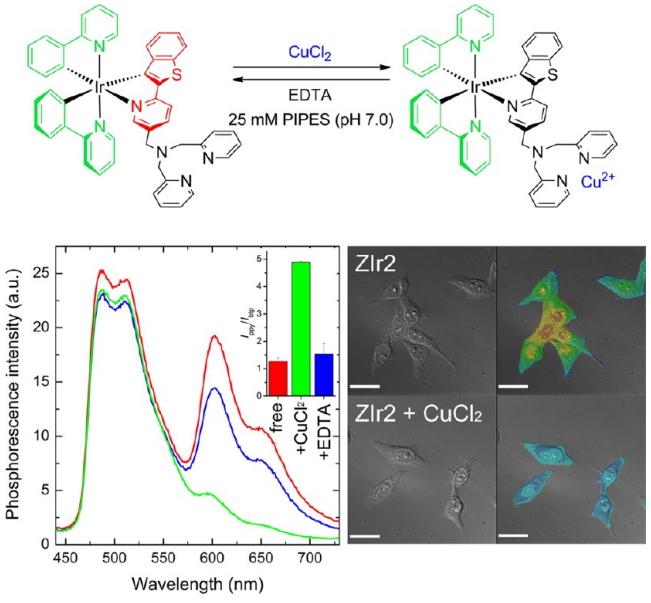

Figure 7. Ratiometric phosphorescence sensor (ZIr2) for cupric ions. The integrated phosphorescence intensities in the ranges of λ = 470–570 nm (green) and 580–700 nm (red) were quantitated. Reprinted with permission from ref 62. Copyright 2011 American Chemical Society.

One disadvantage of using the phosphorescent probe for live cell imaging is photoinduced cytotoxicity. IC_{50} values reach 8.6 and 0.91 μM for A549 (5 h incubation at 37 °C) and HeLa (12 h incubation at 37 °C) cells, respectively.[63] It is speculated that the observed toxicity is due to photosensitization of singlet dioxygen ($^1O_2$) by effective energy transfer to the ground-state O_2.[45,143–145] $^1O_2$ is recognized as a highly reactive oxygen species; therefore, photoinduced generation of $^1O_2$ likely results in abnormal cellular function and, eventually, cell death. Because the quantum yield for $^1O_2$ photosensitization of ZIrdfppy is as high as 0.92, future efforts should be focused on reducing the $^1O_2$-induced cytotoxicity. Incorporation of the complex into passivation objects, such as polymer[146,147] and silica[148] nanoparticles, would be a promising approach.

SUMMARY AND CONCLUDING REMARKS

The biosensing application of a series of phosphorescent cyclometalated iridium(III) complexes is here presented. Metal-chelating receptors can readily be introduced into the ligand peripheries of the iridium(III) complexes to create phosphorescence sensors for detection of zinc, cupric, and chromium ions. Alterations in the structures of the C^N ligands produce varying extents of phosphorescence responses to metal ions. Mechanistic investigations establish that a nonradiative PeT process is dominantly responsible for phosphorescence modulation. It is also found that PeT, occurring in the Marcus-normal region, strictly adheres to the thermodynamic criterion dictated by the Rehm–Weller theory. This finding provides an important guideline for creating PeT-based phosphorescence sensors; large responses can be obtained by increasing the driving force for PeT. In addition to PeT, it is suggested that phosphorescence turn-on might result from the effective suppression of nonradiative ILCT transition. The zinc probe based on the cyclometalated iridium(III) complex is cell-permeable when added to the culture media and is localized within the mitochondria of HeLa cells. The zinc-ion-sensing utility has been verified by carrying out phosphorescent visualization of

dx.doi.org/10.1021/ic4013872 | Inorg. Chem. 2014, 53, 1804–1815

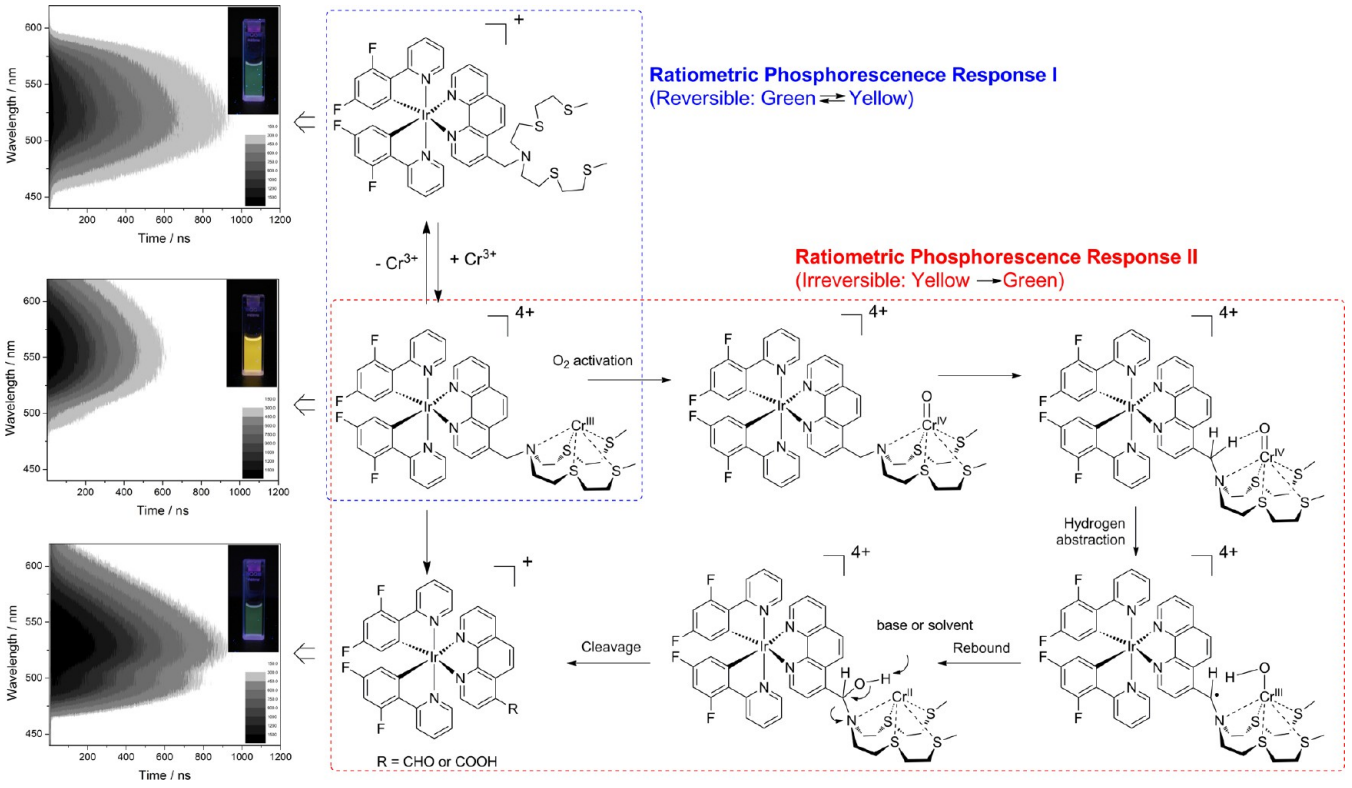

Figure 8. Dual-stage ratiometric responses toward chromium ions. Reprinted with permission from ref 61. Copyright 2012 Wiley-VCH.

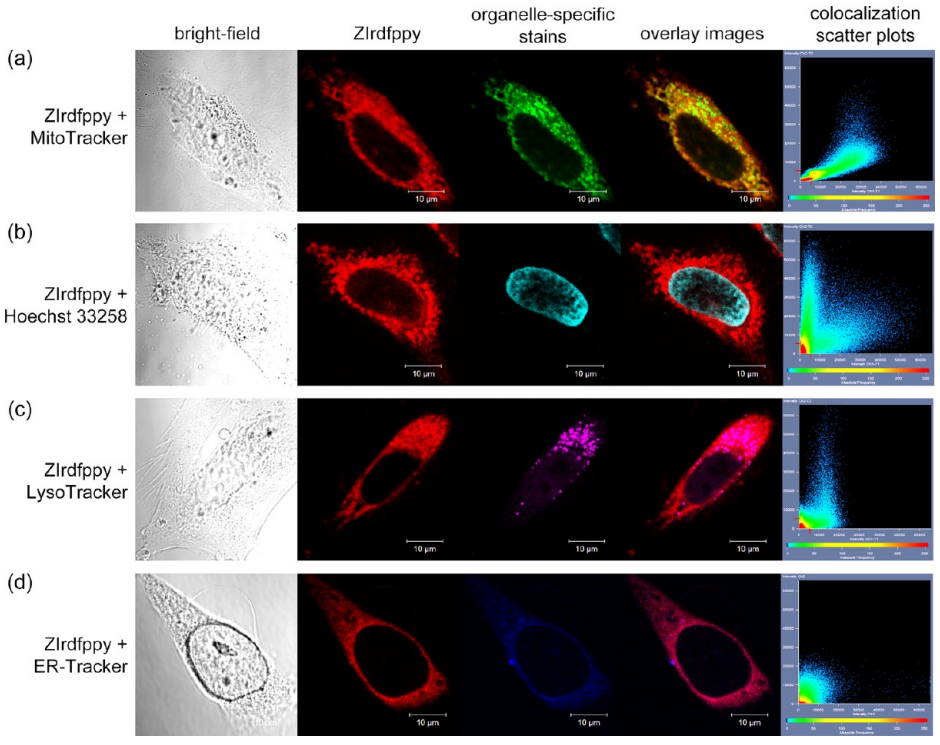

Figure 9. Mitochondrial localization of ZIrdfppy in HeLa cells: (a) 10 μM ZIrdfppy (10 min incubation at 37 °C; λ_{ex} = 405 nm; λ_{em} = 406−550 nm) and 500 nM MitoTracker Deep Red FM (45 min incubation at 37 °C; λ_{ex} = 633 nm; λ_{em} = 637−758 nm); (b) 10 μM ZIrdfppy (10 min incubation at 37 °C; λ_{ex} = 405 nm; λ_{em} = 571−758 nm) and 16 μM Hoechst 33258 (10 min incubation at 37 °C; λ_{ex} = 405 nm; λ_{em} = 406−487 nm); (c) 10 μM ZIrdfppy (10 min incubation at 37 °C; λ_{ex} = 405 nm; λ_{em} = 411−568 nm) and 500 nM LysoTracker Red (2 h incubation at 37 °C; λ_{ex} = 561 nm; λ_{em} = 580−694 nm); (d) 10 μM ZIrdfppy (10 min incubation at 37 °C; λ_{ex} = 405 nm; λ_{em} = 600−750 nm) and 1 μM ER−Tracker Blue−White DPX (30 min incubation at 37 °C; λ_{ex} = 405 nm; λ_{em} = 406−470 nm).

dx.doi.org/10.1021/ic4013872 | Inorg. Chem. 2014, 53, 1804−1815

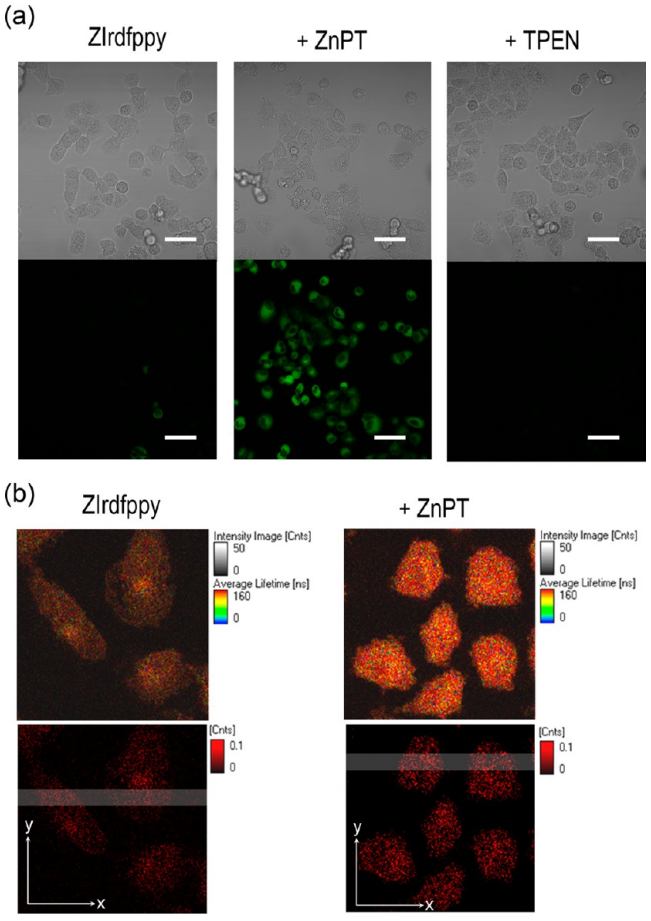

Figure 10. Phosphorescent visualization of intracellular zinc ions in mammalian cells. (a) Confocal laser scanning microscopy images of live A549 cells: left panels, cells incubated with ZIrdfppy; middle panels, cells subsequently treated with $ZnCl_2$/NaPT; right panels, after TPEN addition; top panels, bright-field images; bottom panels, phosphorescence images. Scale bar = 50 μm. (b) Photoluminescence lifetime microscopy images of fixed HeLa cells: left panels, cells incubated with ZIrdfppy; right panels, cells treated with ZIrdfppy and $ZnCl_2$/NaPT; top panels, observed lifetime images; bottom panels, long-lifetime component images. Reprinted with permission from ref 63. Copyright 2011 American Chemical Society.

intracellular zinc ions in mammalian cells. Despite the successes, our studies present the essentials for future research to addressing the disadvantages in the utilization of phosphorescence biosensors based on cyclometalated iridium(III) complexes: (1) The low molar absorbance in the visible region should be improved in order to facilitate imaging in vivo. (2) The redox potentials need to be precisely adjusted to maximize the DR values. (3) Photosensitization of cytotoxic $^1O_2$ has been suggested as being a potential disadvantage for live cell applications; thus, further work to reduce this photoinduced cytotoxicity is required.

■ ASSOCIATED CONTENT

Supporting Information

Experimental details, cyclic voltammograms, correlation between the band-gap energies and redox gaps, optical responses of 50 μM ZIrdfppy to 5 equiv of $ZnCl_2$ at various pHs, thermally assisted intracellular entry of 10 μM ZIrdfppy into HeLa cells, and photophysical and electrochemical data for iridium(III) complexes. This material is available free of charge via the Internet at http://pubs.acs.org.

■ AUTHOR INFORMATION

Corresponding Authors

*E-mail: odds2@khu.ac.kr.
*E-mail: wwnam@ewha.ac.kr.

Notes

The authors declare no competing financial interest.

■ ACKNOWLEDGMENTS

This work was supported by the CRI (W.N.), GRL (Grant 2010-00353 to W.N.), and WCU program (Grant R31-2008-000-10010-0 to W.N.) from the National Research Foundation of Korea and by the Kyung Hee University (Grant KHU-20130385 to Y.Y.).

■ REFERENCES

(1) Tsien, R. Y. *Biochemistry* **1980**, *19*, 2396−2404.
(2) Grynkiewicz, G.; Poenie, M.; Tsien, R. Y. *J. Biol. Chem.* **1985**, *260*, 3440−3450.
(3) Nolan, E. M.; Lippard, S. J. *Acc. Chem. Res.* **2009**, *42*, 193−203.
(4) Kimura, E.; Koike, T. *Chem. Soc. Rev.* **1998**, *27*, 179−184.
(5) Xu, Z.; Yoon, J.; Spring, D. R. *Chem. Soc. Rev.* **2010**, *39*, 1996−2006.
(6) Huang, Z.; Lippard, S. J. *Methods Enzymol.* **2012**, *505*, 445−468.
(7) Torno, K.; Wright, B. K.; Jones, M. R.; Digman, M. A.; Gratton, E.; Phillips, M. *Curr. Microbiol.* **2013**, *66*, 365−367.
(8) Montgomery, C. P.; Murray, B. S.; New, E. J.; Pal, R.; Parker, D. *Acc. Chem. Res.* **2009**, *42*, 925−937.
(9) Mohandessi, S.; Rajendran, M.; Magda, D.; Miller, L. W. *Chem.—Eur. J.* **2012**, *18*, 10825−10829.
(10) Song, C.; Ye, Z.; Wang, G.; Yuan, J.; Guan, Y. *Chem.—Eur. J.* **2010**, *16*, 6464−6472.
(11) Hanaoka, K.; Kikuchi, K.; Kobayashi, S.; Nagano, T. *J. Am. Chem. Soc.* **2007**, *129*, 13502−13509.
(12) Song, B.; Wang, G.; Tan, M.; Yuan, J. *J. Am. Chem. Soc.* **2006**, *128*, 13442−13450.
(13) Wu, J.; Ye, Z.; Wang, G.; Jin, D.; Yuan, J.; Guan, Y.; Piper, J. *J. Mater. Chem.* **2009**, *19*, 1258−1264.
(14) Beeby, A.; Botchway, S. W.; Clarkson, I. M.; Faulkner, S.; Parker, A. W.; Parker, D.; Williams, J. A. G. *J. Photochem. Photobiol. B* **2000**, *57*, 83−89.
(15) Chou, P.-T.; Chi, Y. *Chem.—Eur. J.* **2007**, *13*, 380−395.
(16) Zhao, Q.; Li, F.; Huang, C. *Chem. Soc. Rev.* **2010**, *39*, 3007−3030 and references cited therein.
(17) Ulbricht, C.; Beyer, B.; Friebe, C.; Winter, A.; Schubert, U. S. *Adv. Mater.* **2009**, *21*, 4418−4441.
(18) Schmittel, M.; Lin, H.-W. *Angew. Chem., Int. Ed.* **2007**, *46*, 893−896.
(19) Lanoe, P.-H.; Fillaut, J.-L.; Toupet, L.; Williams, J. A. G.; Le Bozec, H.; Guerchais, V. *Chem. Commun.* **2008**, 4333−4335.
(20) Sato, H.; Tamura, K.; Taniguchi, M.; Yamagishi, A. *Chem. Lett.* **2009**, *38*, 14−15.
(21) Zhao, Q.; Liu, S.; Li, F.; Yi, T.; Huang, C. *Dalton Trans.* **2008**, 3836−3840.
(22) Charbonniere, L. J.; Ziessel, R. F.; Sams, C. A.; Harriman, A. *Inorg. Chem.* **2003**, *42*, 3466−3474.
(23) Li, M.-J.; Chu, B. W.-K.; Zhu, N.; Yam, V. W.-W. *Inorg. Chem.* **2007**, *46*, 720−733.
(24) Lodeiro, C.; Pina, F.; Parola, A. J.; Bencini, A.; Bianchi, A.; Bazzicalupi, C.; Ciattini, S.; Giorgi, C.; Masotti, A.; Valtancoli, B.; Melo, J. S. d. *Inorg. Chem.* **2001**, *40*, 6813−6819.
(25) McFarland, S. A.; Magde, D.; Finney, N. S. *Inorg. Chem.* **2005**, *44*, 4066−4076.
(26) Schmittel, M.; Lin, H. *Inorg. Chem.* **2007**, *46*, 9139−9145.
(27) Shen, Y.; Sullivan, B. P. *Inorg. Chem.* **1995**, *34*, 6235−6236.

(28) Wu, Y.; Jing, H.; Dong, Z.; Zhao, Q.; Wu, H.; Li, F. *Inorg. Chem.* **2011**, *50*, 7412−7420.
(29) Yang, Q.-Z.; Wu, L.-Z.; Zhang, H.; Chen, B.; Wu, Z.-X.; Zhang, L.-P.; Tung, C.-H. *Inorg. Chem.* **2004**, *43*, 5195−5197.
(30) Watanabe, S.; Ikishima, S.; Matsuo, T.; Yoshida, K. *J. Am. Chem. Soc.* **2001**, *123*, 8402−8403.
(31) Kimura, E.; Wada, S.; Shionoya, M.; Takahashi, T.; Iitaka, Y. *J. Chem. Soc., Chem. Commun.* **1990**, 397−398.
(32) Tang, W.-S.; Lu, X.-X.; Wong, K. M.-C.; Yam, V. W.-W. *J. Mater. Chem.* **2005**, *15*, 2714−2720.
(33) Zhao, Q.; Cao, T.; Li, F.; Li, X.; Jing, H.; Yi, T.; Huang, C. *Organometallics* **2007**, *26*, 2077−2081.
(34) Ho, M.-L.; Cheng, Y.-M.; Wu, L.-C.; Chou, P.-T.; Lee, G.-H.; Hsu, F.-C.; Chi, Y. *Polyhedron* **2007**, *26*, 4886−4892.
(35) Guerchais, V.; Fillaut, J.-L. *Coord. Chem. Rev.* **2011**, *255*, 2448−2457.
(36) Chen, Z.-q.; Bian, Z.-q.; Huang, C.-h. *Adv. Mater.* **2010**, *22*, 1534−1539.
(37) Lowry, M. S.; Bernhard, S. *Chem.—Eur. J.* **2006**, *12*, 7970−7977.
(38) Chi, Y.; Chou, P.-T. *Chem. Soc. Rev.* **2010**, *39*, 638−655.
(39) Dixon, I. M.; Collin, J.-P.; Sauvage, J.-P.; Flamigni, L.; Encinas, S.; Barigelletti, F. *Chem. Soc. Rev.* **2000**, *29*, 385−391.
(40) You, Y.; Nam, W. *Chem. Soc. Rev.* **2012**, *41*, 7061−7084.
(41) Flamigni, L.; Barbieri, A.; Sabatini, C.; Ventura, B.; Barigelletti, F. *Top. Curr. Chem.* **2007**, *281*, 143−203.
(42) Zhang, K. Y.; Li, S. P.-Y.; Zhu, N.; Or, I. W.-S.; Cheung, M. S.-H.; Lam, Y.-W.; Lo, K. K.-W. *Inorg. Chem.* **2010**, *49*, 2530−2540.
(43) Li, C.; Yu, M.; Sun, Y.; Wu, Y.; Huang, C.; Li, F. *J. Am. Chem. Soc.* **2011**, *133*, 11231−11239.
(44) Li, S. P.-Y.; Tang, T. S.-M.; Yiu, K. S.-M.; Lo, K. K.-W. *Chem.—Eur. J.* **2012**, *18*, 13342−13354.
(45) Moromizato, S.; Hisamatsu, Y.; Suzuki, T.; Matsuo, Y.; Abe, R.; Aoki, S. *Inorg. Chem.* **2012**, *51*, 12697−12706.
(46) Lo, K. K.-W.; Leung, S.-K.; Pan, C.-Y. *Inorg. Chim. Acta* **2012**, *380*, 343−349.
(47) Lee, P.-K.; Liu, H.-W.; Yiu, S.-M.; Louie, M.-W.; Lo, K. K.-W. *Dalton Trans.* **2011**, *40*, 2180−2189.
(48) Shi, H.; Sun, H.; Yang, H.; Liu, S.; Jenkins, G.; Feng, W.; Li, F.; Zhao, Q.; Liu, B.; Huang, W. *Adv. Funct. Mater.* **2013**, *23*, 3268−3276.
(49) Yang, H.; Li, L.; Wan, L.; Zhou, Z.; Yang, S. *Inorg. Chem. Commun.* **2010**, *13*, 1387−1390.
(50) Jiang, W.; Gao, Y.; Sun, Y.; Ding, F.; Xu, Y.; Bian, Z.; Li, F.; Bian, J.; Huang, C. *Inorg. Chem.* **2010**, *49*, 3252−3260.
(51) Ruggi, A.; Reinhoudt, D. N.; Velders, A. H. *Bioinorg. Med. Chem.* **2011**, 383−406.
(52) Zhao, Q.; Huang, C.; Li, F. *Chem. Soc. Rev.* **2011**, *40*, 2508−2524.
(53) Lo, K. K.-W.; Louie, M.-W.; Zhang, K. Y. *Coord. Chem. Rev.* **2010**, *254*, 2603−2622.
(54) Lo, K. K.-W.; Tsang, K. H.-K.; Sze, K.-S.; Chung, C.-K.; Lee, T. K.-M.; Zhang, K. Y.; Hui, W.-K.; Li, C.-K.; Lau, J. S.-Y.; Ng, D. C.-M.; Zhu, N. *Coord. Chem. Rev.* **2007**, *251*, 2292−2310.
(55) Lo, K. K.-W.; Zhang, K. Y.; Li, S. P.-Y. *Pure Appl. Chem.* **2011**, *83*, 823−840.
(56) Lo, K. K.-W. *Top. Organomet. Chem.* **2010**, *29*, 115−158.
(57) Lo, K. K.-W.; Zhang, K. Y. *RSC Adv.* **2012**, *2*, 12069−12083.
(58) Thorp-Greenwood, F. L. *Organometallics* **2012**, *31*, 5686−5692.
(59) Baggaley, E.; Weinstein, J. A.; Williams, J. A. G. *Coord. Chem. Rev.* **2012**, *256*, 1762−1785.
(60) Lo, K. K.-W.; Li, S. P.-Y.; Zhang, K. Y. *New J. Chem.* **2011**, *35*, 265−287.
(61) Han, Y.; You, Y.; Lee, Y.-M.; Nam, W. *Adv. Mater.* **2012**, *24*, 2748−2754.
(62) You, Y.; Han, Y.; Lee, Y.-M.; Park, S. Y.; Nam, W.; Lippard, S. J. *J. Am. Chem. Soc.* **2011**, *133*, 11488−11491.
(63) You, Y.; Lee, S.; Kim, T.; Ohkubo, K.; Chae, W.-S.; Fukuzumi, S.; Jhon, G.-J.; Nam, W.; Lippard, S. J. *J. Am. Chem. Soc.* **2011**, *133*, 18328−18342.
(64) Lee, P.-K.; Law, W. H.-T.; Liu, H.-W.; Lo, K. K.-W. *Inorg. Chem.* **2011**, *50*, 8570−8579.
(65) Araya, J. C.; Gajardo, J.; Moya, S. A.; Aguirre, P.; Toupet, L.; Williams, J. A. G.; Escadeillas, M.; Le Bozec, H.; Guerchais, V. *New J. Chem.* **2010**, *34*, 21−24.
(66) Medina-Castillo, A. L.; Fernández-Sánchez, J. F.; Klein, C.; Nazeeruddin, M. K.; Segura-Carretero, A.; Fernández-Gutiérrez, A.; Graetzel, M.; Spichiger-Keller, U. E. *Analyst* **2007**, *132*, 929−936.
(67) Koren, K.; Dmitriev, R. I.; Borisov, S. M.; Papkovsky, D. B.; Klimant, I. *ChemBioChem* **2012**, *13*, 1184−1190.
(68) Yoshihara, T.; Yamaguchi, Y.; Hosaka, M.; Takeuchi, T.; Tobita, S. *Angew. Chem., Int. Ed.* **2012**, *51*, 4148−4151.
(69) Zhang, S.-J.; Hosaka, M.; Yoshihara, T.; Negishi, K.; Iida, Y.; Tobita, S.; Takeuchi, T. *Cancer Res.* **2010**, *70*, 4490−4498.
(70) Reddy, G. U.; Das, P.; Saha, S.; Baidya, M.; Ghosh, S. K.; Das, A. *Chem. Commun.* **2013**, *49*, 255−257.
(71) Li, C.; Lin, J.; Guo, Y.; Zhang, S. *Chem. Commun.* **2011**, *47*, 4442−4444.
(72) Leung, K.-H.; He, H.-Z.; Ma, V. P.-Y.; Yang, H.; Chan, D. S.-H.; Leung, C.-H.; Ma, D.-L. *RSC Adv.* **2013**, *3*, 1656−1659.
(73) Tang, Y.; Yang, H.-R.; Sun, H.-B.; Liu, S.-J.; Wang, J.-X.; Zhao, Q.; Liu, X.-M.; Xu, W.-J.; Li, S.-B.; Huang, W. *Chem.—Eur. J.* **2013**, *19*, 1311−1319.
(74) Ma, D.-L.; Wong, W.-L.; Chung, W.-H.; Chan, F.-Y.; So, P.-K.; Lai, T.-S.; Zhou, Z.-Y.; Leung, Y.-C.; Wong, K.-Y. *Angew. Chem., Int. Ed.* **2008**, *47*, 3735−3739.
(75) Wang, X.; Jia, J.; Huang, Z.; Zhou, M.; Fei, H. *Chem.—Eur. J.* **2011**, *17*, 8028−8032.
(76) Xiong, L.; Zhao, Q.; Chen, H.; Wu, Y.; Dong, Z.; Zhou, Z.; Li, F. *Inorg. Chem.* **2010**, *49*, 6402−6408.
(77) Liu, X.; Xi, N.; Liu, S.; Ma, Y.; Yang, H.; Li, H.; He, J.; Zhao, Q.; Li, F.; Huang, W. *J. Mater. Chem.* **2012**, *22*, 7894−7901.
(78) Ma, Y.; Liu, S.; Yang, H.; Wu, Y.; Yang, C.; Liu, X.; Zhao, Q.; Wu, H.; Liang, J.; Li, F.; Huang, W. *J. Mater. Chem.* **2011**, *21*, 18974−18982.
(79) Liu, S.; Qiao, W.; Cao, G.; Chen, Y.; Ma, Y.; Huang, Y.; Liu, X.; Xu, W.; Zhao, Q.; Huang, W. *Macromol. Rapid Commun.* **2013**, *34*, 81−86.
(80) Zhou, C.; Shi, Y.; Ding, X.; Li, M.; Luo, J.; Lu, Z.; Xiao, D. *Anal. Chem.* **2013**, *85*, 1171−1176.
(81) Fraga, S.; Karwowski, J.; Sexena, K. M. S. *Handbook of Atomic Data. Physical Science Data*; Elselvier: New York, 1976; Vol. *5*.
(82) Montalti, M.; Credi, A.; Prodi, L.; Gandolfi, M. T. *Handbook of Photochemistry*, 3rd ed.; Taylor & Francis: New York, 2006.
(83) Fantacci, S.; Angelis, F. D. *Coord. Chem. Rev.* **2011**, *255*, 2704−2726.
(84) You, Y.; Park, S. Y. *Dalton Trans.* **2009**, 1267−1282.
(85) Yersin, H.; Finkenzeller, W. J. In *Highly Efficient OLEDs with Phosphorescent Materials*; Yersin, H., Ed.; Wiley-VCH: Weinheim, Germany, 2008; pp 1−89.
(86) Woo, H.; Cho, S.; Han, Y.; Chae, W.-S.; Ahn, D.-R.; You, Y.; Nam, W. *J. Am. Chem. Soc.* **2013**, *135*, 4771−4787.
(87) Tsuboyama, A.; Iwawaki, H.; Furugori, M.; Mukaide, T.; Kamatani, J.; Igawa, S.; Moriyama, T.; Miura, S.; Takiguchi, T.; Okada, S.; Hoshino, M.; Ueno, K. *J. Am. Chem. Soc.* **2003**, *125*, 12971−12979.
(88) Choi, D. W.; Koh, J. Y. *Annu. Rev. Neurosci.* **1998**, *21*, 347−375.
(89) Maret, W. *Biometals* **2009**, *22*, 149−157.
(90) Takeda, A. *Biometals* **2001**, *14*, 343−351.
(91) Frederickson, C. J. *Int. Rev. Neurobiol.* **1989**, *31*, 145−238.
(92) Frederickson, C. J.; Koh, J.-Y.; Bush, A. I. *Nat. Rev. Neurosci.* **2005**, *6*, 449−462.
(93) Yamaguchi, S.; Miura, C.; Kikuchi, K.; Celino, F. T.; Agusa, T.; Tanabe, S.; Miura, T. *Proc. Natl. Acad. Sci. U.S.A.* **2009**, *106*, 10859−10864.
(94) Weiss, J. H.; Sensi, S. L.; Koh, J. Y. *Trends Pharmacol. Sci.* **2000**, *21*, 395−401.
(95) Marcus, R. A.; Eyring, H. *Annu. Rev. Phys. Chem.* **1964**, *15*, 155−196.
(96) Mizukami, S.; Okada, S.; Kimura, S.; Kikuchi, K. *Inorg. Chem.* **2009**, *48*, 7630−7638.

(97) Komatsu, K.; Urano, Y.; Kojima, H.; Nagano, T. *J. Am. Chem. Soc.* **2007**, *129*, 13447−13454.
(98) Qian, W.-J.; Gee, K. R.; Kennedy, R. T. *Anal. Chem.* **2003**, *75*, 3468−3475.
(99) Gee, K. R.; Zhou, Z.-L.; Ton-That, D.; Sensi, S. L.; Weiss, J. H. *Cell Calcium* **2002**, *31*, 245−251.
(100) Sensi, S. L.; Ton-That, D.; Weiss, J. H.; Rothe, A.; Gee, K. R. *Cell Calcium* **2003**, *34*, 281−284.
(101) Woodroofe, C. C.; Masalha, R.; Barnes, K. R.; Frederickson, C. J.; Lippard, S. J. *Chem. Biol.* **2004**, *11*, 1659−1666.
(102) Burdette, S. C.; Lippard, S. J. *Inorg. Chem.* **2002**, *41*, 6816−6823.
(103) Chang, C. J.; Nolan, E. M.; Jaworski, J.; Okamoto, K.; Hayashi, Y.; Sheng, M.; Lippard, S. J. *Inorg. Chem.* **2004**, *43*, 6774−6779.
(104) Goldsmith, C. R.; Lippard, S. J. *Inorg. Chem.* **2006**, *45*, 555−561.
(105) Nolan, E. M.; Burdette, S. C.; Harvey, J. H.; Hilderbrand, S. A.; Lippard, S. J. *Inorg. Chem.* **2004**, *43*, 2624−2635.
(106) Nolan, E. M.; Jaworski, J.; Racine, M. E.; Sheng, M.; Lippard, S. J. *Inorg. Chem.* **2006**, *45*, 9748−9757.
(107) Wong, B. A.; Friedle, S.; Lippard, S. J. *Inorg. Chem.* **2009**, *48*, 7009−7011.
(108) Burdette, S. C.; Frederickson, C. J.; Bu, W.; Lippard, S. J. *J. Am. Chem. Soc.* **2003**, *125*, 1778−1787.
(109) Burdette, S. C.; Walkup, G. K.; Spingler, B.; Tsien, R. Y.; Lippard, S. J. *J. Am. Chem. Soc.* **2001**, *123*, 7831−7841.
(110) Hirano, T.; Kikuchi, K.; Urano, Y.; Higuchi, T.; Nagano, T. *J. Am. Chem. Soc.* **2000**, *122*, 12399−12400.
(111) Walkup, G. K.; Burdette, S. C.; Lippard, S. J.; Tsien, R. Y. *J. Am. Chem. Soc.* **2000**, *122*, 5644−5645.
(112) Zhang, X.-a.; Hayes, D.; Smith, S. J.; Friedle, S.; Lippard, S. J. *J. Am. Chem. Soc.* **2008**, *130*, 15788−15789.
(113) Sensi, S. L.; Ton-That, D.; Sullivan, P. G.; Jonas, E. A.; Gee, K. R.; Kaczmarek, L. K.; Weiss, J. H. *Proc. Natl. Acad. Sci. U.S.A.* **2003**, *100*, 6157−6162.
(114) Dhara, K.; Karan, S.; Ratha, J.; Roy, P.; Chandra, G.; Manassero, M.; Mallik, B.; Banerjee, P. *Chem.—Asian J.* **2007**, *2*, 1091−1100.
(115) Mikata, Y.; Yamashita, A.; Kawamura, A.; Konno, H.; Miyamoto, Y.; Tamotsu, S. *Dalton Trans.* **2009**, 3800−3806.
(116) Tamanini, E.; Katewa, A.; Sedger, L. M.; Todd, M. H.; Watkinson, M. *Inorg. Chem.* **2009**, *48*, 319−324.
(117) Frederickson, C. J.; Kasarskis, E. J.; Ringo, D.; Frederickson, R. E. *J. Neurosci. Methods* **1987**, *20*, 91−103.
(118) Liu, Y.; Zhang, N.; Chen, Y.; Wang, L.-H. *Org. Lett.* **2007**, *9*, 315−318.
(119) Liu, Z.; Zhang, C.; Li, Y.; Wu, Z.; Qian, F.; Yang, X.; He, W.; Gao, X.; Guo, Z. *Org. Lett.* **2009**, *11*, 795−798.
(120) Zhang, Y.; Guo, X.; Si, W.; Jia, L.; Qian, X. *Org. Lett.* **2008**, *10*, 473−476.
(121) Henary, M. M.; Wu, Y.; Fahrni, C. J. *Chem.—Eur. J.* **2004**, *10*, 3015−3025.
(122) Kwon, J. E.; Lee, S.; You, Y.; Baek, K.-H.; Ohkubo, K.; Cho, J.; Fukuzumi, S.; Shin, I.; Park, S. Y.; Nam, W. *Inorg. Chem.* **2012**, *51*, 8760−8774.
(123) Taki, M.; Wolford, J. L.; O'Halloran, T. V. *J. Am. Chem. Soc.* **2004**, *126*, 712−713.
(124) Fahrni, C. J.; Henary, M. M.; VanDerveer, D. G. *J. Phys. Chem. A* **2002**, *106*, 7655−7663.
(125) Henary, M. M.; Fahrni, C. J. *J. Phys. Chem. A* **2002**, *106*, 5210−5220.
(126) Que, E. L.; Domaille, D. W.; Chang, C. J. *Chem. Rev.* **2008**, *108*, 1517−1549.
(127) Chang, C. J.; Jaworski, J.; Nolan, E. M.; Sheng, M.; Lippard, S. J. *Proc. Natl. Acad. Sci. U.S.A.* **2004**, *101*, 1129−1134.
(128) Lim, N. C.; Freake, H. C.; Brueckner, C. *Chem.—Eur. J.* **2005**, *11*, 38−49.
(129) Jiang, P.; Guo, Z. *Coord. Chem. Rev.* **2004**, *248*, 205−229.
(130) Tomat, E.; Lippard, S. J. *Curr. Opin. Chem. Biol.* **2010**, *14*, 225−230.
(131) Nonoyama, M. *Bull. Chem. Soc. Jpn.* **1974**, *47*, 767−768.
(132) Miura, T.; Urano, Y.; Tanaka, K.; Nagano, T.; Ohkubo, K.; Fukuzumi, S. *J. Am. Chem. Soc.* **2003**, *125*, 8666−8671.
(133) Okamoto, K.; Fukuzumi, S. *J. Am. Chem. Soc.* **2004**, *126*, 13922−13923.
(134) Chen, H.-Y.; Yang, C.-H.; Chi, Y.; Cheng, Y.-M.; Yeh, Y.-S.; Chou, P.-T.; Hsieh, H.-Y.; Liu, C.-S.; Peng, S.-M.; Lee, G.-H. *Can. J. Chem.* **2006**, *84*, 309−318.
(135) Goldstein, D. C.; Cheng, Y. Y.; Schmidt, T. W.; Bhadbhade, M.; Thordarson, P. *Dalton Trans.* **2011**, *40*, 2053−2061.
(136) Leslie, W.; Batsanov, A. S.; Howard, J. A. K.; Williams, J. A. G. *Dalton Trans.* **2004**, 623−631.
(137) Liu, T.; Zhang, H.-X.; Xia, B.-H. *J. Organomet. Chem.* **2008**, *693*, 947−956.
(138) Liu, T.; Zhang, H.-X.; Xia, B.-H. *J. Phys. Chem. A* **2007**, *111*, 8724−8730.
(139) Chen, J.-L.; Wu, Y.-H.; He, L.-H.; Wen, H.-R.; Liao, J.; Hong, R. *Organometallics* **2010**, *29*, 2882−2891.
(140) Zhao, N.; Wu, Y.-H.; Wen, H.-M.; Zhang, X.; Chen, Z.-N. *Organometallics* **2009**, *28*, 5603−5611.
(141) Malaiyandi, L. M.; Vergun, O.; Dineley, K. E.; Reynolds, I. J. *J. Neurochem.* **2005**, *93*, 1242−1250.
(142) Atkinson, A.; Khalimonchuk, O.; Smith, P.; Sabic, H.; Eide, D.; Winge, D. R. *J. Biol. Chem.* **2010**, *285*, 19450−19459.
(143) Gao, R.; Ho, D. G.; Hernandez, B.; Selke, M.; Murphy, D.; Djurovich, P. I.; Thompson, M. E. *J. Am. Chem. Soc.* **2002**, *124*, 14828−14829.
(144) Djurovich, P. I.; Murphy, D.; Thompson, M. E.; Hernandez, B.; Gao, R.; Hunt, P. L.; Selke, M. *Dalton Trans.* **2007**, 3763−3770.
(145) Li, S. P.-Y.; Lau, C. T.-S.; Louie, M.-W.; Lam, Y.-W.; Cheng, S. H.; Lo, K. K.-W. *Biomaterials* **2013**, *34*, 7519−7532.
(146) Wu, H.; Yang, T.; Zhao, Q.; Zhou, J.; Li, C.; Li, F. *Dalton Trans.* **2011**, *40*, 1969−1976.
(147) Zhou, Z.; Li, D.; Yang, H.; Zhu, Y.; Yang, S. *Dalton Trans.* **2011**, *40*, 11941−11944.
(148) Lai, C.-W.; Wang, Y.-H.; Lai, C.-H.; Yang, M.-J.; Chen, C.-Y.; Chou, P.-T.; Chan, C.-S.; Chi, Y.; Chen, Y.-C.; Hsiao, J.-K. *Small* **2008**, *4*, 218−224.